Bone Marrow-derived Cells Participate in the Formation of Normal and Neoplastic Lung Stroma

SUSAN D'COSTA[1], LUKE BORST[1] and YONGBAEK KIM[2,3]

[1]Department of Population Health and Pathobiology, College of Veterinary Medicine, North Carolina State University, Raleigh, NC, U.S.A.; [2]Laboratory of Clinical Pathology and [3]Research Institute for Veterinary Science, College of Veterinary Medicine, Seoul National University, Seoul, The Republic of Korea

Abstract. *Background/ Aim: The present study was performed in order to investigate the distribution of transplanted bone marrow-derived cells (BMDCs) in normal and neoplastic tissues. Materials and Methods: A microchimeric mouse model harboring traceable BMDCs was created by injecting labeled BMDCs into adenovirus-expressing Cre (AdenoCre)-infected, irradiated, LSL-K-ras^{G12D} p53$^{fl/fl}$ mice. Results: In the normal mice, transplanted cells were detected in the femur, tibia, lung, heart, kidney and spleen of recipient mice. The transplanted BMDCs were detected predominantly in the connective tissue around the smaller bronchioles of normal lung parenchyma. In the lung tumor-bearing mice, the transplanted BMDCs were detected within the tumor tissue and more abundantly in the connective tissue adjacent to the tumor mass. Conclusion: This study provides morphological evidence of a microchimeric experimental system that may promote further research into the role of BMDCs in the carcinogenic process and for the development of a novel therapy aimed at targeting stromal cells and, eventually, tumor growth.*

Lung cancer is the leading cause of cancer-related death worldwide, accounting for 26 to 28% of annual cancer deaths in the United States, and is the second most frequently diagnosed type of cancer in men and women (1). Lung tumors typically arise from the epithelium of conducting airways or alveolar parenchyma. The process of carcinogenesis and tumor progression is significantly influenced by tumor-associated stroma (TAS), providing tissue microenvironments (2). TAS consists of extracellular matrix and a variety of cells that work in concert, such as myofibroblasts, tumor-associated macrophages, mast cells, neutrophils, and endothelial cells (3).

In the past decade, several cell populations of bone marrow-derived stem cells (BMDCs) were suggested to form TAS; two of these populations are mesenchymal stem cells (MSCs) and hematopoietic stem cells (HSCs) (4). These BMDCs can be mobilized into the bloodstream, and recruited to tumors, where they may promote tumor growth and progression. However, the role of BMDCs in forming TAS remains controversial. Several studies have shown a significant contribution of BMDCs to tumor vascularization (5), while others have reported that the presence of BMDCs in TAS is artifactual rather than physiological (6). Morphologically, the amount of TAS is significantly increased in advanced adenocarcinoma, compared to earlier stages of carcinogenesis, indicating that TAS formation is significantly enhanced at the progression stage.

Conditional double-mutant *K-ras*^{G12D} *p53*$^{fl/fl}$ mice have been developed as a model to study lung tumor development (7, 8). A lox-stop-lox (LSL) cassette in the first intron of the *K-ras* gene prevents the expression of the mutant allele until the stop elements are removed by the activity of Cre recombinase (Cre). Following administration of recombinant adenovirus expressing Cre recombinase (Adeno-Cre), these mice go on to develop lung tumors due to loss of *p53* and induction of expression of the oncogenic form of *K-ras* (8). The goal of this study was to determine if BMDCs are the source of lung TAS, and to examine their role in the pulmonary carcinogenic process using a microchimeric mouse lung cancer model that harbors traceable BMDCs in *LSL-K-ras*^{G12D} *p53*$^{fl/fl}$ mice.

Materials and Methods

Breeding and genotyping of transgenic mice. Double-mutant LSL-*K-ras*^{G12D} *p53*$^{fl/fl}$ mice (Duke University, Durham, NC, USA) were used as recipients for BMDCs. *K-ras*^{G12D} *p53*$^{fl/fl}$ mice were

Correspondence to: Dr. Yongbaek Kim, The Laboratory of Clinical Pathology, College of Veterinary Medicine, Seoul National University,1 Gwanak-ro, Gwanak-gu, Seoul 151-742, The Republic of Korea. Tel: +82 28801273, Fax: +82 28731213, e-mail: yongbaek@snu.ac.kr

Key Words: Lung cancer, mouse mode, bone marrow-derived cells, green fluorescent protein.

crossed and offspring were genotyped using tail clip DNA and *Kras* F1, *Kras* R1 and SD5' primers. Primer sequences were provided by the laboratory of Dr. David Kirsch (Duke University): *Kras* F1: 5'-GTCTTTCCCCAGCACAGT GC-3', *Kras* R1: 5'-CTCTTGC CTACGCCACCAGCTC-3', SD5': 5'-AGCTAGCCACCATGGC TTGAGTAAGTCTGCA-3. Polymerase chain reaction (PCR) with wild-type primers (*Kras* F1 and *Kras* R1) produced a 650 bp product, while amplification with mutant primers (*Kras* R1 and SD5') resulted in a 550 bp product. Donor *C57BL/6-Tg(CAG-EGFP) 131Osb/LeySopJ* transgenic mice were obtained from Jackson Laboratories Inc. (Bar Harbor, Maine, USA). Hemizygous males for *Tg(CAG-EGFP) 131Osb* were crossed with wild-type females and green fluorescent protein (GFP)-positive offspring were identified using a GFP Flashlight (NightSea LLC., Andover, MA, USA) and appropriate goggles. Mice were housed in the Laboratory Animal Resources at the College of Veterinary Medicine, North Carolina State University. Animal experiments were reviewed and approved by the Institutional Animal Care and Use Committee, North Carolina State University.

Depletion of endogenous BMDCs by whole-body radiation. A week prior to radiation, mice were started on a Nutra-Gel diet (Bio-serve, Frenchtown, NJ, USA) and antibiotic (Trimethoprim-sulfa) containing, autoclaved water. Recipient C57BL/6 mice were weighed on the day of irradiation and after it was confirmed that the recipient mice were in good health, their food was removed on the day of irradiation, but water was provided. Mice were placed in an autoclaved radiation disc (Braintree Scientific, Inc. Braintree, MA, USA) and transported to the radiation room. A total of eight mice were irradiated with a single dosage of 12 Gy using a Varian Clinac 1800 instrument (Varian Associate, Inc., Palo Alto, CA, USA). Mice were returned to their autoclaved cages containing Nutra-Gel and antibiotic water.

Isolation and transplantation of BMDCs to irradiated mice. The femur and tibia were collected from donor C57BL/6 mice (14 weeks of age) and the bone marrow was flushed out using medium (RPMI 1640 with 2% FBS, 10 units/ml of heparin and antibiotics). The clumps of cells were agitated and the cell suspension passed through a 23-gauge needle and strained through a 40-μm cell strainer. Cells were centrifuged, counted and resuspended in serum-free medium. Within 24 h of radiation, mice received 5×10^6 donor BMDCs. The mice were transplanted with BMDCs or vehicle *via* the lateral tail vein. Two non-irradiated mice were used as controls for each experiment. The mice receiving RPMI were euthanized on the third day following radiation. Mice that received BMDCs were monitored daily for up to two weeks for food consumption, weight gain, impairment of mobility or inability to eat, drink, defecate or urinate, rough hair coat, diarrhea, bacterial infection *etc*. Mice were euthanized if weight loss was greater than 15%, or they exhibited any of the above signs of distress. Samples collected from all mice and fixed in 10% neutral-buffered formalin (NFB) included: stomach, spleen, lung, liver, intestine, femur and tibia. Prior to processing, bone samples were de-calcified and samples were processed in paraffin and stained with hematoxylin and eosin (H&E) using standard techniques.

Intranasal administration of virus for the development of lung tumors. *K-ras*^{G12D} *p53*$^{fl/fl}$ (n=12) and *K-ras*$^{+/+}$ *p53*$^{fl/fl}$ (n=5) mice were infected with 5.5 to 7.5×10^6 plaque forming units (PFU) of Ad5CMVCre (AdenoCre) virus (Gene Transfer Vector Core, University of Iowa, Ames, IA, USA) at 7 to 12 weeks of age. The virus was pipetted into minimum essential medium (MEM), CaCl2 was added to the MEM-virus mix, which was then incubated at room temperature for 20 min. Mice were anesthetized *via* intraperitoneal injection of a mixture of ketamine and xylazine. In a biosafety hood, the mouse was placed in the hand, ventral side up, such that the head was positioned above its feet. Holding the end of a pipet tip over the opening of one nostril, the virus was dispensed dropwise until the entire volume of virus had been inhaled. The mouse was placed on a recirculating warm water pad to recover. Mice were infected with a volume ranging from 50-75 μl per mouse. The mice were weighed every week and at 12 to16 weeks post-infection the mice were euthanized. The liver, lung, kidney spleen, heart, femur and tibia samples were collected, fixed overnight in 10% NBF, and processed in paraffin for histological sectioning using standard techniques. H&E-stained sections were evaluated by a single pathologist for the presence and type (adenoma or carcinoma) of lung tumor.

Production of a microchimera mouse lung cancer model harboring GFP-labeled BMDCs. *K-ras*^{G12D} *p53*$^{fl/fl}$ mice (7 to 10 weeks of age) were anesthetized and administered 7.5×10^6 PFU per mouse of AdenoCre virus according to the above protocol. Infected mice were observed every day and weighed once a week. In the first trial mice were irradiated at 10 days post-infection, while in a second trial, mice were irradiated at 11 weeks post-infection according to the above procedure. Within 24 h of irradiation, mice received donor BMDCs from *C57BL/6-Tg (CAG-EGFP)131Osb/LeySopJ* mice (4 or 6 weeks of age). Isolation and transplantation of GFP- BMDCs was carried out according to the above procedure. *K-ras*^{G12D} *p53*$^{fl/fl}$ recipient mice were injected with 7.5×10^6 BMDCs.

Detection of GFP-labeled BMDC in mouse tissues. Recipient mice were euthanized at days 4-15 following radiation and examined for tumors. The heart, liver, lung, femur, tibia, kidney and spleen were collected and placed in fixatives. The femur and tibia were de-calcified prior to paraffin embedding. The formalin-fixed samples were embedded in paraffin and used for H&E staining and immunohistochemical detection of GFP. Following de-paraffinization, antigen retrieval was performed in a pressure chamber in the presence of citrate buffer at pH 6. Endogenous peroxidase was quenched by immersing the sections in 3% H_2O_2 in deionized water for 10 min (de-calcified bone tissue) or 30 min (other tissues). GFP-positive donor cells were identified in microchimeras using a rabbit polyclonal GFP antibody (Abcam, Cambridge, MA, USA), and Vectastain ABC kit and DAB substrate obtained from Vector Laboratories, Inc. (Burlingame, CA, USA). Sections were counter-stained with hematoxylin, then dehydrated and mounted with Permount. GFP mice were used as positive controls for immunohistochemistry.

Lung tissues from individuals that were identified as chimeras were also processed for direct observation of GFP. For direct GFP detection, a piece of lung was placed in 4% paraformaldehyde and frozen in OCT medium (Ted Pella, Inc., Redding, CA, USA) and sectioned. Cryosections were warmed to room temperature, hydrated in PBS and mounted in Vectamount containing 4',6-diamidino-2-phenylindole (DAPI) (Vector Laboratories, Inc.). Transgenic GFP and *K-ras*^{G12D} *p53*$^{fl/fl}$ mice with no transplantation were used as positive and negative controls, respectively. Slides were observed under epifluorescence using a MX6000 Series

Table I. *Lung tumor production in mice infected with AdenoCre virus.*

Genotype	Post-infection (weeks)	Total	Positive	Negative	Percentage
K-ras^{G12D} *p53*$^{fl/fl}$	15-16	5	3	2	60
	12-13	7	7	0	100
	Total	12	10	2	83
K-ras$^{+/+}$ *p53*$^{fl/fl}$	16	1	0	1	0
	12	4	0	4	0
	Total	5	0	5	0

microscope (Meiji Techno UK Ltd, Axbridge, UK) and digital images were obtained using Infinity Analyze Software (Lumenera Corp. Ottawa, ON, Canada). The DAPI and GFP images were merged using Adobe Photoshop.

Results

Production of mice with different genetic backgrounds. Genotypes of the offspring mice were determined using PCR. Breeding pairs of *K-ras*^{G12D} *p53*$^{fl/fl}$ mice generated offspring with *K-ras*^{G12D} *p53*$^{fl/fl}$ (55%) and *K-ras*$^{+/+}$ *p53*$^{fl/fl}$ (45%) genotypes. Breeding between hemizygous *C57BL/6-Tg(CAG-EGFP)131Osb/LeySopJ* males and wild-type females produced wild-type and GFP-positive offsprings. These mice with different genetic backgrounds were used for further experiments.

Transplantation of bone marrow cells following irradiation. Compared to bone marrow from age-matched unirradiated mice (Figure 1a) a single dose of 12-Gy radiation significantly reduced cell numbers in femur and tibia (Figure 1b), with complete bone marrow depletion. In the irradiated mice that received transplants of BMDCs, the bone marrow was moderately cellular (Figure 1c), indicating the effective replacement of bone marrow cells by the transplanted BMDCs.

Induction of lung tumors by intranasal administration of AdenoCre virus. None of the *K-ras*$^{+/+}$ *p53*$^{fl/fl}$ mice infected with AdenoCre virus developed lung tumors at 12-16 weeks following infection (Figure 2a), while 10 out of 12 (83%) *K-ras*^{G12D} *p53*$^{fl/fl}$ mice developed lung tumors (Table I). Multiple lung tumors ranging from adenoma to adenocarcinoma were observed in the majority of *K-ras*^{G12D} *p53*$^{fl/fl}$ mice (Figure 2b). All tumors appeared to be bronchiolar alveolar carcinomas that formed near the bronchioles. The mice sacrificed at 16 weeks post-infection with AdenoCre virus had more advanced tumors than mice at 12 to 13 weeks post-infection. Lung tumors exhibited tubuloalveolar growth with occasional solid areas composed of pleomorphic neoplastic cells. The neoplastic epithelial cells were columnar to cuboidal and often demonstrated criteria of malignancy, including marked anisokaryosis, anisocytosis, prominent and multiple nucleoli and frequent, often bizarre, mitotic figures (Figure 2c).

Fate of transplanted BMDCs in the mouse tissues. At four weeks post-infection with AdenoCre virus, GFP-positive donor cells were detected by immunohistochemistry in one out of the five *K-ras*^{G12D} *p53*$^{fl/fl}$ recipient mice. Numerous donor cells were detected in the bone marrow of femur and tibia and the lung, heart, spleen and kidneys. In the recipient lung, GFP-positive cells were detected predominantly in the connective tissue around the smaller bronchioles.

At 12-14 weeks post-infection with AdenoCre virus, GFP-positive cells were immunohistochemically detected in two out of the four *K-ras*^{G12D} *p53*$^{fl/fl}$ injected mice. Following transplantation, GFP-labeled donor cells were detected in the femur (Figure 3a and b), tibia, lung (Figure 3c and d), heart, kidney and spleen. A large number of donor-derived cells were identified in the lung of the recipient mice. The presence of the GFP-expressing cells in the lung parenchyma was confirmed by direct detection of GFP fluorescence in frozen sections. Within the normal lung parenchyma, GFP-labeled cells were detected predominantly in the connective tissue around the smaller bronchioles (Figure 4a). In tumor-bearing lung, GFP-expressing, donor-derived cells were detected in TAS as well as surrounding the tumor tissue (Figure 4b).

Discussion

Using the microchimeric model system harboring GFP-labeled bone marrow cells, we illustrated the distribution of the cellular components derived from transplanted BMDCs within multiple parenchymal organs including lung, heart, kidney, spleen, and bone marrow. Additionally, the cells derived from the transplanted BMDCs participated in the formation of TAS. The identity of the cells derived from the transplanted BMDCs warrants further study. Bone marrow is a reservoir of two distinct populations of stem cells, HSCs and MSCs. HSCs are the source of blood cells that are subsequently released to

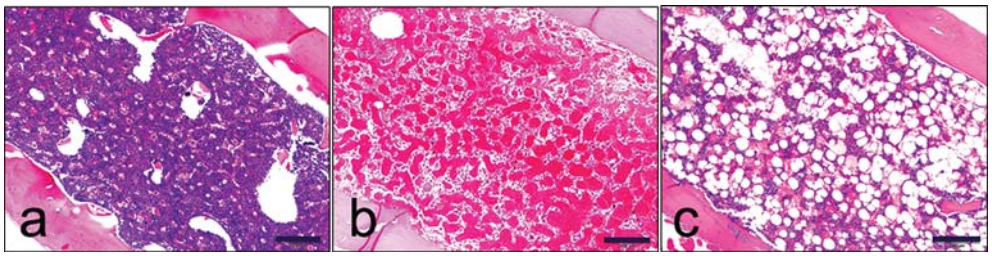

Figure 1. *Bone marrow of femurs from a: A non-irradiated control mouse showing normal bone marrow cellularity; b: a mouse irradiated with single dose of 12-Gy radiation followed by intravenous injection of vehicle, showing completely depleted bone marrow cells; c: a recipient mouse irradiated with a single dose of 12-Gy radiation followed by intravenous injection of bone marrow-derived donor cells, exhibiting re-populated bone marrow cells. Hematoxylin and eosin. Bars=200 μm.*

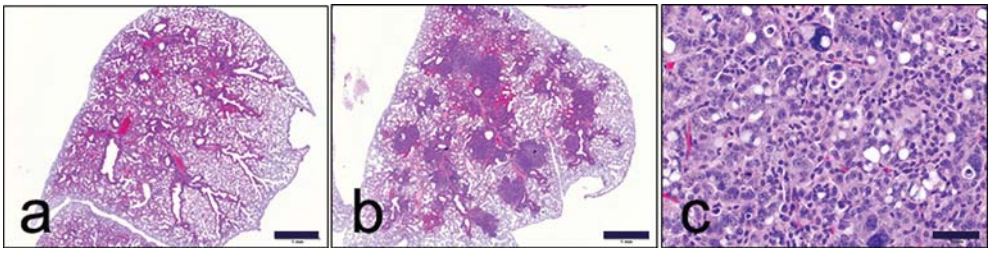

Figure 2. *a: Lung from a K-ras$^{+/+}$ p53$^{fl/fl}$ mouse at 12 weeks post-infection with AdenoCre virus, exhibiting normal pulmonary architecture. b: Lung from a LSL-K-ras^{G12D} p53$^{fl/fl}$ mouse at 12 weeks post-infection with AdenoCre virus, showing multiple hypercellular areas representing neoplastic foci. c: Higher magnification of lung tumor tissue from a LSL-K-ras^{G12D} p53$^{fl/fl}$ mouse at 16 weeks post-infection with AdenoCre virus, showing highly cellular area composed of pleomorphic neoplastic cells. Hematoxylin and eosin. Bars (a, b) =1 mm; (c) =50 μm.*

circulation. Bone marrow MSCs represent 0.01-0.001% of all nucleated cells and have been shown to generate various stromal cells found in bone, adipose tissues, cartilage, and smooth muscle (9). Some of these cells migrate to peripheral tissues and become resident stromal cells in multiple organs. Our data showed that the BMDCs migrated to the multiple parenchymal tissues and became resident stromal cells. In the lung, most of the migrated BMDCs were observed in the connective tissue around the small bronchioles. Normally, fibroblasts, endothelial cells, pericytes and inflammatory cells, including macrophages, are found in the pulmonary connective tissue around small bronchioles. Although the identity of the BMDCs was not determined in the present study, they were mesenchymal cells rather than macrophages based on their morphological features. It has been suggested that the role of MSCs in tissue growth and re-generation relies on both the integration of MSCs into the tissues and on the secretory activity of these cells (10).

Recent insights revealed that cancer is not only a disease of the transformed cells but is also influenced and dependent on the microenvironment regulated by stromal cells (2). Tumor progression and metastasis involves extensive interactions of the aggressive cancer cells with the stromal component (11). TAS consists of extracellular matrix and a variety of cells that work in concert. It has been suggested that both resident and bone marrow-derived MSCs play a profound role in the formation of TAS (11). Myofibroblasts are an important component of TAS and are thought to arise from several cell types including tissue resident MSCs or fibroblasts, and bone marrow-derived MSCs (12). Abundance of myofibroblasts in the tumor stroma is associated with clincopathological features such as invasive growth, lymph node metastasis, and regional recurrence (13). One study suggested that bone marrow-derived MSCs contribute up to 25% of the myofibroblast population in the tumor stroma in a mouse model of pancreatic insulinoma (14). In our study, GFP-labeled BMDCs were characterized as isolated, elongated cells lacking organization. These cells were present within the tumor *in situ*, but were more abundant at the periphery of the tumor. The findings suggest that BMDCs may play a significant role at the sites of expansion and metastasis along the periphery of the developing tumor.

Cytokines and growth factors produced by tumors may participate in the recruitment of resident and distant respondent cells such as MSCs. MSCs intravenously injected *via* the tail vein of tumor-bearing mice migrated to the

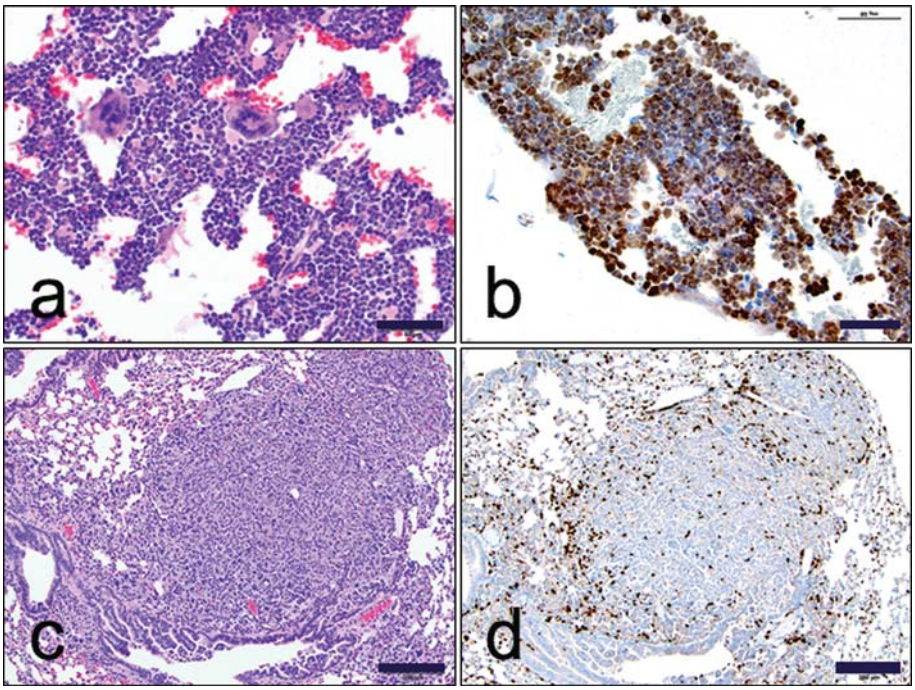

Figure 3. *Immunohistochemical detection of the transplanted, green fluorescent protein (GFP)-expressing cells. a, b: Bone marrow from a LSL-K-ras^{G12D} p53$^{fl/fl}$ recipient mouse with intravenously-injected GFP- bone marrow-derived cells (BMDCs). c, d: Lung with tumor tissue from a LSL-K-ra^{sG12D} p53$^{fl/fl}$ recipient mouse with intravenous injection of BMDCs. Note the positively (brown)-labeled GFP-BMDCs in the bone marrow and stroma adjacent to lung tumors in the recipient mouse. Hematoxylin and eosin (a, c) and immunohistochemistry for GFP (b, d). Bars (a, b) =100 μm; (c, d)=200 μm.*

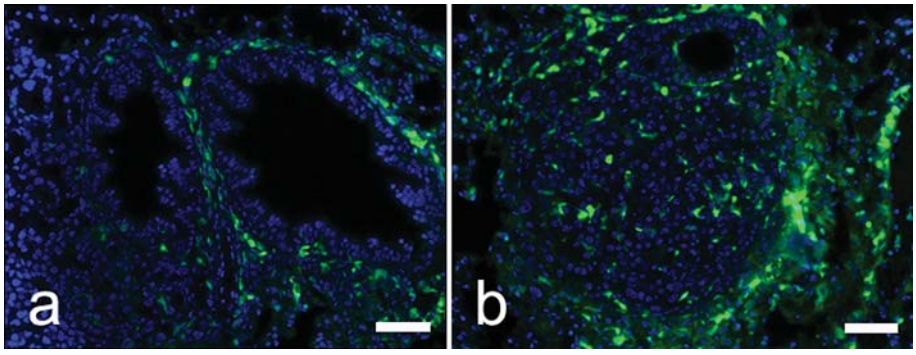

Figure 4. *Direct detection of the transplanted, green fluorescent protein (GFP)-expressing donor-derived cells using an epifluorescence microscope. a: Normal lung parenchyma from a LSL-K-ras^{G12D} p53$^{fl/fl}$ mouse injected with GFP-expressing bone marrow-derived cells (BMDCs). Note the infiltration of GFP-BMDCs within the stroma supporting normal bronchioles. b: Tumor-bearing lung parenchyma from a LSL-K-ras^{G12D} p53$^{fl/fl}$ mouse injected with GFP-BMDCs. Note the infiltration of GFP-BMDCs primarily within the tumor-associated stroma. Nuclear stain with DAPI. Bars=200 μm.*

xenografts, derived from several cancer cell lines (15). Anticancer treatment may affect the recruitment of MSCs to tumor tissue. Irradiated tumors showed an increase in MSC recruitment compared to unirradiated tumors (16). Migration of MSCs may result from a dynamic interplay involving cytokines from cancer cells and chemokine receptor up-regulation on MSCs (17). In our study, BMDCs were more abundant in the tumor tissue compared to the normal pulmonary parenchyma. These findings indicate that tumor tissue secretes chemoattractants that recruit BMDCs.

Alternatively, factors may enhance the expression levels of chemokine receptor in BMDCs, facilitating their migration to tumor tissue. The innate cancer-homing capabilities of MSCs have been considered as a valuable tool for treating malignant diseases. Elucidation of the underlying mechanism is necessary for the development of a novel therapeutic strategy using MSCs.

In conclusion, this study provides background information including morphological evidence, promoting further research into dissecting mechanisms that control migration of BMDCs to tumor tissues, and the interactions between BMDCs and tumor cells and/or resident stromal cells facilitating tumor progression. Moreover, the microchimeric system established in this study, may be a useful tool for investigating novel therapies that aim to target stromal cells and, eventually, tumor growth.

Acknowledgements

This project was supported by the Department of Defense Lung CancerResearch Program Concept Award (Grant #: LC090309). Authors thank Dr. David G. Kirsch(Duke University) for providing the *K-ras*^{G12D} *p53*$^{fl/fl}$ mice, Dr. Adam Moeser for microscope use, Laura Edwards for tail vein injections and Karen Gaither for assistance with the mice.

References

1 Siegel R, Naishadham D and Jemal A: Cancer statistics, 2013. CA Cancer J Clin *63*: 11-30, 2013.

2 Tlsty TD and Coussens LM: Tumor stroma and regulation of cancer development. Annu Rev Pathol *1*: 119-150, 2006.

3 Li H, Fan X and Houghton J: Tumor microenvironment: The role of the tumor stroma in cancer. J Cell Biochem *101*: 805-815, 2007.

4 Taketo MM: Role of bone marrow-derived cells in colon cancer: Lessons from mouse model studies. J Gastroenterol *44*: 93-102, 2009.

5 Peters BA, Diaz LA, Polyak K, Meszler L, Romans K, Guinan EC, Antin JH, Myerson D, Hamilton SR, Vogelstein B, Kinzler KW and Lengauer C: Contribution of bone marrow-derived endothelial cells to human tumor vasculature. Nat Med *11*: 261-262, 2005.

6 Purhonen S, Palm J, Rossi D, Kaskenpaa N, Rajantie I, Yla-Herttuala S, Alitalo K, Weissman IL and Salven P: Bone marrow-derived circulating endothelial precursors do not contribute to vascular endothelium and are not needed for tumor growth. Proc Natl Acad Sci USA *105*: 6620-6625, 2008.

7 Jackson EL, Olive KP, Tuveson DA, Bronson R, Crowley D, Brown M and Jacks T: The differential effects of mutant *p53* alleles on advanced murine lung cancer. Cancer Res *65*: 10280-10288, 2005.

8 Kirsch DG, Grimm J, Guimaraes AR, Wojtkiewicz GR, Perez BA, Santiago PM, Anthony NK, Forbes T, Doppke K, Weissleder R and Jacks T: Imaging primary lung cancers in mice to study radiation biology. Int J Radiat Oncol Biol Phys *76*: 973-977, 2010.

9 Charbord P: Bone marrow mesenchymal stem cells: Historical overview and concepts. Hum Gene Ther *21*: 1045-1056, 2010.

10 Salem HK and Thiemermann C: Mesenchymal stromal cells: Current understanding and clinical status. Stem Cells *28*: 585-596, 2010.

11 Sleeman JP, Christofori G, Fodde R, Collard JG, Berx G, Decraene C and Ruegg C: Concepts of metastasis in flux: The stromal progression model. Semin Cancer Biol *22*: 174-186, 2012.

12 De Boeck A, Narine K, De Neve W, Mareel M, Bracke M and De Wever O: Resident and bone marrow-derived mesenchymal stem cells in head and neck squamous cell carcinoma. Oral Oncol *46*: 336-342, 2010.

13 De Wever O, Demetter P, Mareel M and Bracke M: Stromal myofibroblasts are drivers of invasive cancer growth. Int J Cancer *123*: 2229-2238, 2008.

14 Direkze NC, Hodivala-Dilke K, Jeffery R, Hunt T, Poulsom R, Oukrif D, Alison MR and Wright NA: Bone marrow contribution to tumor-associated myofibroblasts and fibroblasts. Cancer Res *64*: 8492-8495, 2004.

15 Gao Y, Yao A, Zhang W, Lu S, Yu Y, Deng L, Yin A, Xia Y, Sun B and Wang X: Human mesenchymal stem cells overexpressing pigment epithelium-derived factor inhibit hepatocellular carcinoma in nude mice. Oncogene *29*: 2784-2794, 2010

16 Kim SM, Oh JH, Park SA, Ryu CH, Lim JY, Kim DS, Chang JW, Oh W and Jeun SS: Irradiation enhances the tumor tropism and therapeutic potential of tumor necrosis factor-related apoptosis-inducing ligand-secreting human umbilical cord blood-derived mesenchymal stem cells in glioma therapy. Stem Cells *28*: 2217-2228, 2010.

17 Smith H, Whittall C, Weksler B and Middleton J: Chemokines stimulate bi-directional migration of human mesenchymal stem cells across bone marrow endothelial cells. Stem Cells Dev *21*: 476-486, 2012.

Received January 8, 2013
Revised January 26, 2013
Accepted January 28, 2013